UDC 539.12.04.621.384.653

THE USE OF PLASMA-BASED DEPOSITION WITH ION IMPLANTATION TECHNOLOGY TO PRODUCE SUPERHARD MOLYBDENUM-BASED COATINGS IN A MIXED (C_2H_2+N_2) ATMOSPHERE

O.V. Sobol'[1], A.A. Andreev[2], R.P. Mygushchenko[1], V.M. Beresnev[3], A.A. Meylekhov[1], A.A. Postelnyk[1], S.A. Kravchenko[1], Taha A. Tabaza[4], Safwan M. Al-Qawabah[4], Ubeidulla F. Al-Qawabeha[5], V.A. Stolbovoy[2], I.V. Serdyuk[2], D.A. Kolesnikov[6], M.G. Kovaleva[6]

[1]National Technical University "Kharkiv Polytechnical Institute", Kharkov, Ukraine
E-mail: sool@kpi.kharkov.ua;
[2]National Science Center "Kharkov Institute of Physics and Technology", Kharkov, Ukraine
E-mail: aandreev@kipt.kharkov.ua;
[3]V.N. Karazin Kharkiv National University, Kharkov, Ukraine;
[4]Al-Zaytoonah University, Amman 11733, Jordan;
[5]Tafila Technical University, At-Tafilah, P O Box 179, Tafila, 66110, Jordan;
[6]Belgorod State National Research University, Belgorod, Russia

The influence of the pressure of a mixed gaseous atmosphere (80%C_2H_2+20%N_2) and the supply of a high-voltage negative potential in a pulsed form on the elemental and phase composition, structure and physico-mechanical characteristics of the vacuum-arc molybdenum-based coatings. It is shown that in the temperature deposition range 400…550 °C as a result of plasma-chemical reactions, the maximum nitrogen atoms content in the coating does not exceed 1.5 at.%. It is found, that at the maximum pressure of $P_{C_2H_2+N_2} = 2.3 \cdot 10^{-1}$ Pa when the γ-MoC phase is formed, an superhard state of 50.5 GPa (at a constant potential -200 V, without additional high-voltage pulse action) and 51.1 GPa (at a constant potential -200 V, with additional high-voltage pulse action) is reached.

INTRODUCTION

Structural engineering is in recent years the main method for obtaining coating materials with unique structural states [1, 2] and functional properties [3–5]. Non-equilibrium conditions for the coatings formation allow stabilizing high-temperature phases [6], nanostructured high-hard composite materials [7, 8], multi-element (high-entropy) materials based on simple crystal lattices (bcc, fcc, hcp [9]). Such materials have good tribological characteristics [10], high hardness and resistance to radiation impact [11].

To control the energy characteristics of the coatings deposition, the plasma-based deposition with ion implantation technology has proven itself [12, 13]. With this technology, the supply of a negative high voltage potential of 1…2 kV in a pulsed mode (with millisecond duration) to the substrate leads to grain refinement [13], stress relaxation [14] and, in many cases, to a large misorientation of crystal growth directions [15]. In this case, the use of high-voltage pulses makes it possible to increase the functional properties of not only single-layer but also multilayer systems (for example, Ti/TiN [16], Ag/Zn [17], etc.). Also, the positive effect of the increase in properties under high-voltage pulse action is noted during the reactive deposition of TiN coatings in a gas mixture of 80%N_2+20%H_2 [18]. Considering the above (pulse stimulation of deposition in a gas mixture), however, the greatest influence of high-voltage pulse stimulation should be expected during the reactive deposition of coatings in a gas mixture containing nitrogen and carbon compounds. Comparative experiments have shown that the use of a mixture of gases C_2H_2 and N_2 is most advanced for the creation of coatings [19]. The coatings obtained in the C_2H_2+N_2 gas mixture have high performance characteristics [20], low friction coefficient [21], high mechanical properties [22, 23], and also for a number of systems, it is possible to obtain an advanced "nitride-DLC" composition [24, 25].

It should be taken into account that at high temperatures the nitrides of most transition metals are less thermodynamically stable than the corresponding carbides. As a result, nitrides interact with carbon to form the corresponding carbides or carbonitrides and release nitrogen gas. With increasing temperature, the process of nitrides interaction with carbon accelerates and is directed towards formation of the corresponding carbide and gaseous nitrogen.

Molybdenum nitrides are unstable in a carbon-containing medium at temperatures above 800 °C ($2Mo_2N+2C = 2Mo_2C+N_2$ reaction is realized [26]). The process of carbides formation can be further activated if the predominant formation is carried out in a carbon-and nitrogen-containing plasma with a high degree of ionization, which is achieved by using a vacuum arc method. In this case, the temperature of preferential carbide formation can be significantly reduced.

The aim of this work is to analyze the influence of the pressure (from 80%C_2H_2+20%N_2 gas mixture), as well as the high-voltage pulse potential on the phase composition, structure and physico-mechanical characteristics of Mo-based vacuum-arc coatings.

1. EXPERIMENTAL DETAILS

The coatings were obtained by vacuum-arc method on the modernized unit "Bulat-6". The pressure of the working (C_2H_2+N_2) atmosphere during deposition was P = (0.23…2.3)·10^{-1} Pa. The deposition rate was about 2 nm/s. Deposition was carried out on the surface of samples 20x20x2 mm from steel 12Cr18Ni10Ti (analog of stainless steel SS 321) austenitic steel (Ra = 0.09 μm).

MChVP molybdenum was used as cathode material. During deposition, a constant negative bias potential (U_b) of -200 V was fed to the substrate.

In a number of experiments, a pulsed mode (with a duration of 7 μs) was used supplying a high-voltage potential to the substrate with the value U_{ip} = -2000 V to stimulate accelerated diffusion without significant surface heating.

The gas mixture (C_2H_2+N_2) was created using a gas mixture generator (GMG) (Fig. 1) and is implemented in two stages. At the first stage, a preliminary cyclical blowing of the mixing chamber by one of the gases included in the mixture is carried out. In the second stage, a direct mixture is created by sequentially gases supplying to the mixing chamber up to corresponding to a specified percentage of them in the mixture partial pressures.

The main advantages of this method are: it is no need to ensure the equality of the inlet pressure of gases and their dosing in batches of equal volume [27].

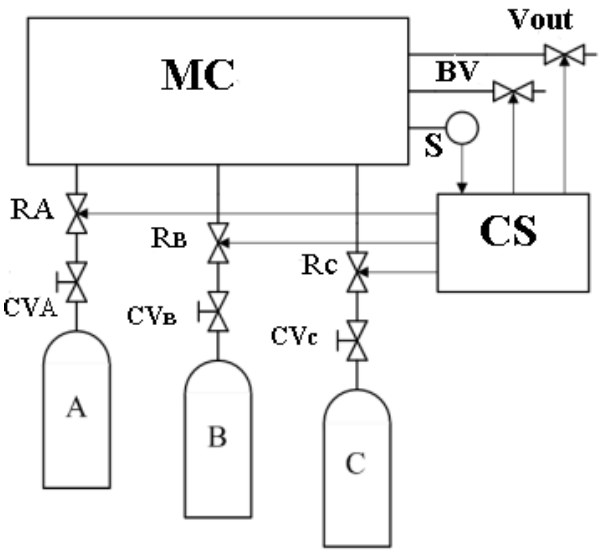

Fig. 1. Block diagram of GMG: A, B, C – cylinders with gases; MC – mixing chamber; CS – control system; R_A, R_B, R_C – reducers; CV_A, CV_B, CV_C – controlled valves; BV – blow down valve; V_{out} – the output valve; S – pressure sensor

The phase-structure analysis was carried out by X-ray diffractometry in Cu-kα radiation using a DRON-4. To monochromatize radiation, a graphite monochromator was used, which was installed in a secondary beam (in front of the detector). The study of the phase composition, structure (texture, substructure) was carried out using traditional X-ray diffractometry techniques by analyzing the position, intensity, and shape of the diffraction reflection profiles. To identify the diffractograms, the tables of the international diffraction data center "Powder Diffraction File" were used.

The substructural characteristics (microdeformation <ε> and the crystallite size L) were determined by the approximation method, i. e. varying the width of the diffraction reflections from several orders of reflections [28].

The hardness was measured by a microindentation method with a diamond indentor (Vickers pyramid) at 50 g loads. The study was performed on a 402MVD microhardness testing device designed by Instron Wolpert Wilson Instruments.

The elemental coating composition was studied with the Quanta 200 3D Electron-Ion Scanning Microscope.

To determine the adhesive strength, a Revetest scratch tester (CSM Instruments) was used. Diamond spherical indenter "Rockwell C" with a curvature radius of 200 μm, were applied with a continuously increasing load. At the same time, the power of the acoustic emission (AE) signal, the friction coefficient and penetration depth of the indenter, as well as the magnitude of the normal load were recorded.

2. RESULTS AND DISCUSSION

An energy-dispersive analysis of the elemental composition of the coatings obtained in the gas mixture (80%C_2H_2+20%N_2) plasma did not reveal the presence of nitrogen in coatings obtained at low pressure P = (2.3…5.3)·10^{-2} Pa. In coatings obtained at the highest pressure 0.23 Pa (optimal for achieving the highest mechanical properties [9]), the nitrogen content was about 1.5%.

It should be noted that the pulsed high-voltage potential supply (for stimulation of physicochemical reactions on the surface during deposition of coatings) leads to a decrease in the relative content of nitrogen atoms to a zero value even at high pressures of the working atmosphere.

Analysis of the phase composition and structural state of the coatings was carried out by X-ray diffraction method and showed that at low pressures MoC phase with a cubic crystal lattice (structural type NaCl) and texture with the axis [111] (Fig. 2,a) is formed. The lattice period is a = 0.4563 nm. The average crystallite size of the MoC phase (in the direction of the texture axis [111]) is about 20 nm.

At higher pressure and low energy (because of its collision loss in the inter electrode gap), a γ-MoC phase (PDF 45-1015) with a hexagonal crystal lattice is formed (see Fig. 2,a, spectra 2 and 3). At higher pressures (when forming a more complex type of crystal lattice and in the absence of texture), the crystallites have a smaller average size (about 9.5 nm).

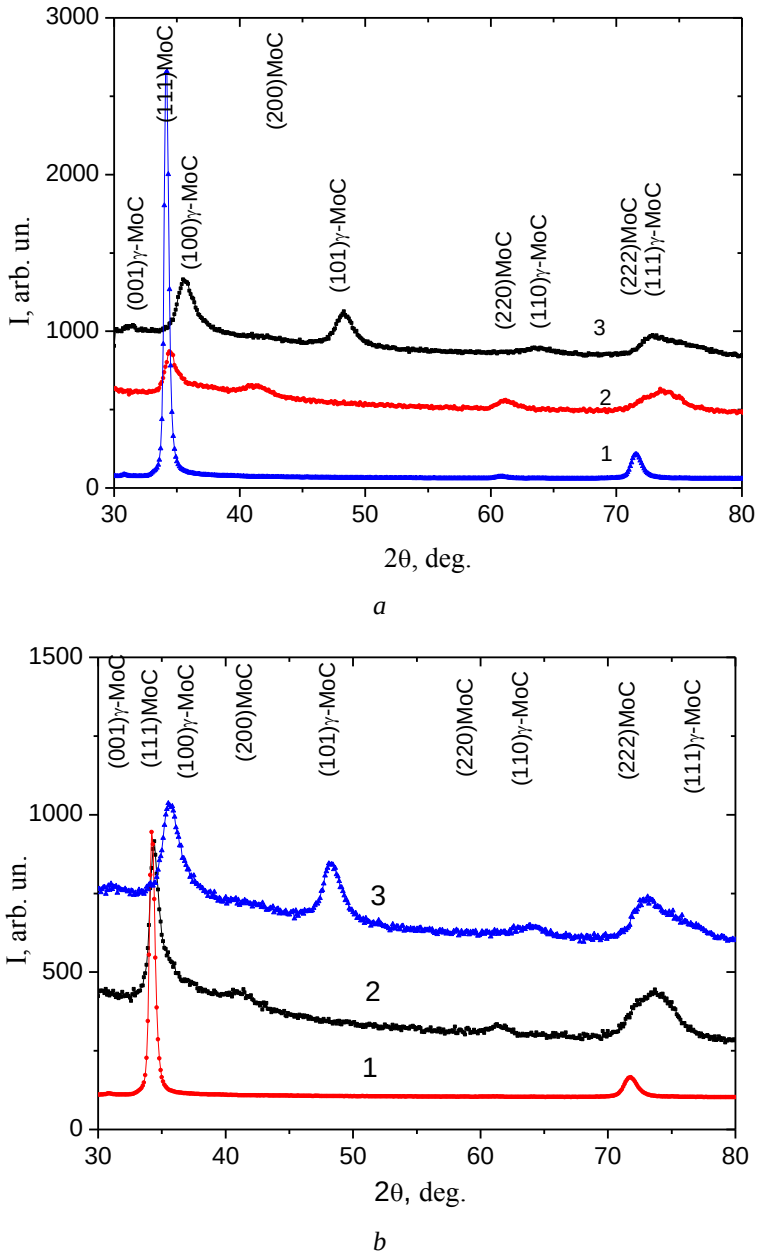

Fig. 2. X-ray diffraction spectra of coatings obtained in a mixed 80%C_2H_2+20%N_2 atmosphere at U_b = -200 V (a) and U_b = -200 V, U_{ip} = -2000 V (b). The pressure during deposition was: 1 – 2.3·10^{-2} Pa; 2 – 5.3·10^{-2} Pa; 3 – 0.23 Pa

The additional use of U_{ip} during coating deposition does not lead to a qualitative change in the phase composition (see Fig. 2,b). In this case, the U_{ip} supply leads to a change in the lattice period and the average crystallite size. The lattice period of the MoC phase is 0.4552 nm. This value is less than in coatings obtained without U_{ip}. The reasons for this decrease in the period are: the relative decrease in the carbon atoms content in octahedral interstices and the partial relaxation of the compression stressed state [29]. The average crystallite size is 16 nm.

At high pressures (5.2·10^{-2}…2.3·10^{-1} Pa) a γ-MoC phase is formed with crystallites of medium size about 9 nm.

Thus, the use of U_{ip} leads to a decrease in the average crystallites size. This may be due to an increase in the crystallites nucleation sites [29] and a decrease in the lattice period (i. e., formation of a denser state).

Hardness, adhesion resistance, friction coefficient and acoustic emission were studied as functional physico-mechanical characteristics.

The most universal mechanical characteristic of coatings was hardness [9]. Fig. 3 shows the generalized hardness dependence on P during deposition without U_{ip} (curve 1) and when using U_{ip} (curve 2). As can be seen, the greatest hardness is achieved at the highest pressure 0.23 Pa. According to the XRD-data, this corresponds to the formation of a single-phase (γ-MoC phase with a hexagonal lattice) state. In this case, nanometer-sized crystallites are formed (about 9.5 nm (without U_{ip}) and 9 nm (with U_{ip})).

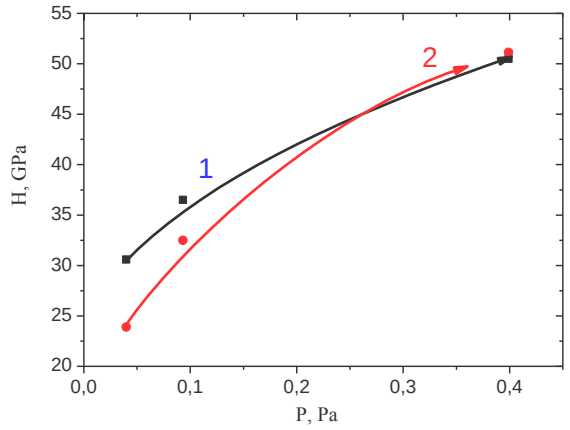

Fig. 3. Dependence of the coatings microhardness on the pressure of 80%C_2H_2+20%N_2 gas mixture at U_b = -200 V (1) and U_b = -200 V, U_{ip} = -2000 V (2)

It should be noted that at low pressures hardness is higher in coatings obtained without U_{ip} (see Fig. 3). Higher values of hardness under the action of U_{ip} are achieved at the highest pressure 0.23 Pa during deposition.

Adhesion strength determined by the scratch test method is relatively large. The critical load of coating (L_c5) damage is 47.2 N (without U_{ip}) and 46.2 N (with U_{ip}). At a critical load, cracks appear on the coating surface, which shape is shown in Fig. 4.

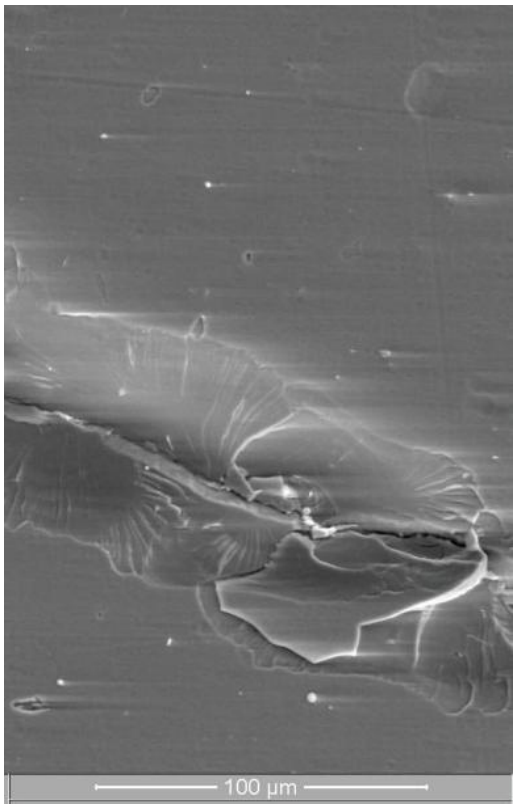

Fig. 4. The surface crack formed in the coating after critical loading

To record the acoustic emission (AE) signal and the friction coefficient, the tests were performed under the following conditions: the load on the indenter increased from 0.9 to 70 N, the speed of the indenter movement was 1 mm/min, the scratch length was 10 mm, the load rate was 6.91 N/min, the signal discreteness frequency was 60 Hz, the power of the acoustic emission signal was 9 dB. Fig. 5 shows the dependence of the change in the average values of the acoustic emission amplitude (see spectrum 1, Fig. 5) and the friction coefficient (see spectrum 2, Fig. 5) on the load on the indenter and the displacement length for scratch testing.

It can be seen that the curve of the change in the acoustic signal power has a peak at 20 N (coating without U_{ip}, Fig. 5,a) and several similar peaks for the second type coating (see Fig. 5,b). In this case, for the second coating, such peaks are less intense. The presence of such peaks, as is known [10], indicates the defects formation in the coating material (cracks). Thus, in the first type coatings, larger cracks are formed, but in a relatively smaller amount. In the second type coatings, smaller defects are formed, but in a larger amount. If we compare it with the structural data, we see that in the first type coatings the average grain size is larger than in the second type coatings. Thus, if the appearance and propagation of a crack occurs at weakened places near the grain-crystallite boundary, then such a mechanism is in good agreement with the results obtained during the study of acoustic emission.

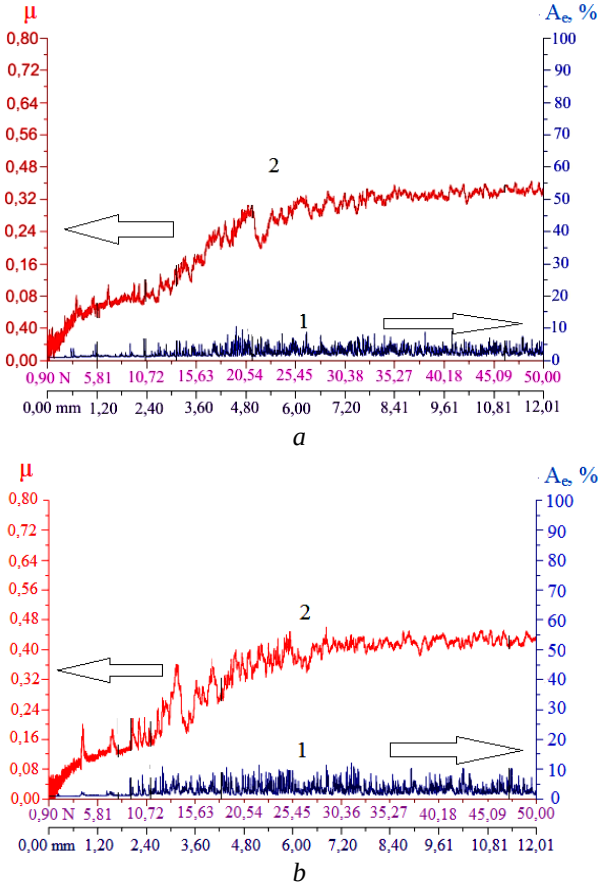

Fig. 5. Change in averaged values of the acoustic emission amplitude (spectrum 1), and the friction coefficient (spectrum 2) during scratch testing of coatings obtained at U_b = -200 V (a) and U_b = -200 V, U_{ip} = -2000 V (b) (P = 0.23 Pa)

It can be seen that the friction coefficient varies with the formation of such cracks. This is determined by the peaks (along with the cracks formed according to acoustic emission data) appearing from the friction

dependence on the displacement length during scratch testing.

The friction coefficient in the initial section (before the first cracks are formed) at a load of about 10 N is 0.14 (for the first type coatings) and 0.13 (for the second type coatings). In areas close to the coatings damage (at a load of more than 30 N), the friction coefficient for coatings of both types is about 0.4.

CONCLUSIONS

It is determined that molybdenum carbide is formed in the temperature range of 400…550 °C during deposition as a result of plasma chemical reactions in the coating formed in the C_2H_2+N_2 gas mixture. Thus, carbide-based coatings are more effective for high-temperature applications, when nitrides are less stable than carbides.

When the gaseous atmospheric composition is 80%C_2H_2+20%N_2, the maximum content of nitrogen atoms in the coating does not exceed 1.5 at.%. The supply of a pulsed high-voltage potential (for stimulation of physicochemical reactions on the surface during deposition of coatings) leads to a decrease in the relative content of nitrogen atoms in the coating.

At a low pressure $P = 2.3 \cdot 10^{-1}$ Pa, a MoC phase is formed with a cubic (structural type NaCl) crystal lattice and texture with the axis [111].

At a higher pressure $P = 5.2 \cdot 10^{-2} \ldots 2.3 \cdot 10^{-1}$ Pa, a γ-MoC phase is formed with a hexagonal lattice. The supply of a high-voltage potential in a pulsed form leads to a decrease in the average size of the crystallites, an increase in their misorientation and stress relaxation.

It is found, that at the maximum pressure $P_{C_2H_2+N_2}=2.3 \cdot 10^{-1}$ Pa when the γ-MoC phase is formed, an superhard state of 50.5 GPa (at a constant potential of -200 V, without additional high-voltage pulse action) and 51.1 GPa (at a constant potential -200 V, with additional high-voltage pulse action) is reached.

REFERENCES

1. A.E. Barmin, O.V. Sobol', A.I. Zubkov, L.A. Mal'tseva. Modifying effect of tungsten on vacuum condensates of iron // *The Physics of Metals and Metallography.* 2015, N 116(7), p. 706-710.

2. O.V. Sobol'. Structural engineering vacuum-plasma coatings interstitial phases // *Journal of Nano- and Electronic Physics.* 2016, N 8(2), p. 02024.

3. A.E. Barmin, A.I. Zubkov, A.I. Il'inskii. Structural features of the vacuum condensates of iron alloyed with tungsten // *Functional Materials*. 2012, N 19(2), p. 256-259.

4. B.D. Morton, H. Wang, R.A. Fleming, M. Zou. Nanoscale surface engineering with deformation-resistant core-shell nanostructures // *Tribology Letters*. 2011, N 42(1), p. 51-58.

5. M. Bourebia, L. Laouar, H. Hamadache & S. Dominiakn. Improvement of surface finish by ball burnishing: approach by fractal dimension // *Surface Engineering*. 2017, N 33(4), p. 255-262.

6. O.V. Sobol'. The influence of nonstoichiometry on elastic characteristics of metastable β-WC_{1-x} phase in ion plasma condensates // *Technical Physics Letters*. 2016, N 42(9), p. 909-911.

7. V.I. Ivashchenko, S.N. Dub, P.L. Scrynskii, A.D. Pogrebnjak, O.V. Sobol', G.N. Tolmacheva, V.M. Rogoz, A.K. Sinel'chenko. Nb-Al-N thin films: Structural transition from nanocrystalline solid solution nc-(Nb, Al)N into nanocomposite nc-(Nb, Al)N/a-AlN // *Journal of Superhard Materials*. 2016, N 38(2), p. 103-113.

8. A.D. Pogrebnjak, O.V. Bondar, G. Abadias, V. Ivashchenko, O.V. Sobol', S. Jurga, E. Coy. Structural and mechanical properties of NbN and Nb-Si-N films: Experiment and molecular dynamics simulations // *Ceramics International*. 2016, N 42(10), p. 11743-11756.

9. A.D. Pogrebnjak, I.V. Yakushchenko, G. Abadias, P. Chartier, O.V. Bondar, V.M. Beresnev, Y. Takeda, O.V. Sobol', K. Oyoshi, A.A. Andreyev, B.A. Mukushev. The effect of the deposition parameters of nitrides of high-entropy alloys (TiZrHfVNb)N on their structure, composition, mechanical and tribological properties // *Journalof superhard materials*. 2013, N 35(6), p. 356-368.

10. S.N. Grigoriev, O.V. Sobol', V.M. Beresnev, I.V. Serdyuk, A.D. Pogrebnyak, D.A. Kolesnikov, U.S. Nemchenko. Tribological characteristics of (TiZrHfVNbTa)N coatings applied using the vacuum arc deposition method // *Journal of Friction and Wear*. 2014, N 35(5), p. 359-364.

11. A.A. Andreev, V.N. Voyevodin, O.V. Sobol', V.F. Gorban', G.N. Kartmazov, V.A. Stolbovoy, V.V. Levenets, D.V. Lysan. Regularities in the effect of model ion irradiation on the structure and properties of vacuum-arc nitride coatings // *Problems of Atomic Science and Technology.* 2013, N 87(5), p. 142-146.

12. W. Olbrich and G. Kampschulte. Superimposed pulse bias voltage used in arc and sputter technology // *Surf. Coat. Technol*. 1993, N 59, p. 274-280.

13. S.H.N. Lim, D.G. McCulloch, M.M. Bilek, and D.R. McKenzie. Minimisation of intrinsic stress in titanium nitride using a cathodic arc with plasma immersion ion implantation // *Surf. Coat. Technol.* 2003, N 174, p. 76-80.

14. M.M.M. Bilek, D.R. McKenzie, R.N. Tarant, et al. Plasma based ion implantation utilising a cathodic arc plasma // *Surf. Coat. Technol*. 2003, N 156, p. 136-142.

15. O.V. Sobol', A.A. Andreev, S.N. Grigor'ev, V.F. Gorban', M.A. Volosova, S.V. Aleshin, V.A. Stolbovoy. Physical characteristics, structure and stress state of vacuum-arc tin coating, deposition on the substrate when applying high-voltage pulse during the deposition // *Problems of Atomic Science and Technology*. 2011, N 4, p. 174-177.

16. F. Bermeo, J.P. Quintana, A. Kleiman, F. Sequeda, A. Márquez. 1020 steel coated with Ti/TiN by cathodic arc and ion implantation // *Journal of Physics.* 2017, N 792(1), p. 1-6.

17. A. Gao, R. Hang, P.K. Chu. Recent advances in anti-infection surfaces fabricated on biomedical implants by plasma-based technology // *Surface and Coatings Technology*. 2017, N 312, p. 2-6.

18. M. Cisternas, F. Mellero, M. Favre, H. Bhuyan, E. Wyndham. TiN Coatings on titanium substrates using

plasma assisted ion implantation // *Journal of Physics: Conference Series*. 2015, N 591(1).

19. G. Strnad, D. Biro, I. Vida-Simitl. Contributions to processing of self-lubricated, nanocomposite wear resistant coatings by reactive UM magnetron co-sputtering // *Materials and Technologies – 4th International Conference on Materials and Manufacturing Technologies*. 2007, N 23, p. 197-200.

20. J.J. Guan, H.Q. Wang, L.Z. Qin, B. Liao, H. Liang, B. Li. Phase transitions of doped carbon in CrCN coatings with modified mechanical and tribological properties via filtered cathodic vacuum arc deposition // *Nuclear Instruments and Methods in Physics Research. Section B: Beam Interactions with Materials and Atoms.* 2017, N 397, p. 86-91.

21. B. Lin, L. Wang, Q. Wan, S. Yan, Z. Wang, B. Yang, D. Fu. Low. Friction-coefficient TiBCN nanocomposite coatings prepared by cathode arc plasma deposition // *Plasma Science and Technology*. 2015, N 17(3), p. 221-227.

22. Y.-S. Yang, T.-P. Cho, H.-W. Ye. The effect of deposition parameters on the mechanical properties of Cr-C-N coatings // *Surface and Coatings Technology*. 2014, N 259, p. 141-145.

23. W. Tillmann, S. Momeni. Tribological development of TiCN coatings by adjusting the flowing rate of reactive gases // *Journal of Physics and Chemistry of Solids*. 2016, N 90, p. 45-53.

24. Y. Cai, R.Y. Wang, H.D. Liu, C. Luo, Q. Wan, Y. Liu, H. Chen, Y.M. Chen, Q.S. Mei, B. Yang. Investigation of (Ti:N)-DLC coatings prepared by ion source assisted cathodic arc ion-plating with varying Ti target currents // *Diamond and Related Materials.* 2016, N 69, p. 183-190.

25. H.-L. Huang, Y.-Y. Chang, J.-X. Liu, M.-T. Tsai, C.-H. Lai. Antibacterial activity and cell compatibility of TiZrN, TiZrCN, and TiZr-amorphous carbon coatings // *Thin Solid Films*. 2015, N 596, p. 111-117.

26. Г.В. Самсонов. *Нитриды*. Киев: «Наукова думка», 1969, 380 с.

27. Ю.А. Сысоев, И.В. Сердюк, А.В. Доломанов, Д.В. Ковтеба. Генератор газовых смесей для ионно-плазменных технологий // *Вопросы атомной науки и техники*. 2017, № 2(108), с. 178-183.

28. H.P. Klug and L.E. Alexander. X-Ray Diffraction Procedures for Polycrystalline and Amorphous Materials, 2nd edn. // *John Wiley and Sons, Inc.* New York. 1974, 992 p.

29. O.V. Sobol'. Control of the structure and stress state of thin films and coatings in the process of their preparation by ion-plasma methods // *Physics of the Solid State*. 2011, N 53(7), p. 1464-1473.

Article received 27.11.2017

ИСПОЛЬЗОВАНИЕ ТЕХНОЛОГИИ КОНДЕНСАЦИИ ПРИ ИОННОЙ БОМБАРДИРОВКЕ ДЛЯ ПОЛУЧЕНИЯ СВЕРХТВЕРДЫХ ПОКРЫТИЙ НА ОСНОВЕ МОЛИБДЕНА В СМЕШАННОЙ (C_2H_2+N_2) АТМОСФЕРЕ

О.В. Соболь, А.А. Андреев, Р.П. Мигущенко, В.М. Береснев, А.А. Мейлехов, А.А. Постельник, С.А. Кравченко, Taha A. Tabaza, Safwan M. Al-Qawabah, Ubeidulla F. Al-Qawabeha, В.А. Столбовой, И.В. Сердюк, Д.А. Колесников, М.Г. Ковалева

Для вакуумно-дуговых покрытий на основе молибдена изучено влияние давления смешанной газовой атмосферы (80%C_2H_2+20%N_2) и высоковольтного отрицательного потенциала (подаваемого на подложку в импульсной форме) на элементный и фазовый состав, структуру и физико-механические характеристики формируемого материала. Показано, что в температурном интервале подложки при осаждении 400…550 °С в результате плазмохимических реакций максимальное содержание атомов азота в покрытии не превышает 1,5 ат.%. Выявлено, что при наибольшем давлении $P_{C_2H_2+N_2} = 2{,}3\cdot10^{-1}$ Па, когда формируется фаза γ-MoC, достигается сверхтвердое состояние 50,5 ГПа (при постоянном потенциале -200 В, без дополнительного высоковольтного импульсного потенциала) и 51,1 ГПа (при постоянном потенциале -200 В, с дополнительным высоковольтным импульсным потенциалом).

ВИКОРИСТАННЯ ТЕХНОЛОГІЇ КОНДЕНСАЦІЇ ПРИ ІОННОМУ БОМБАРДУВАННІ ДЛЯ ОТРИМАННЯ НАДТВЕРДИХ ПОКРИТТІВ НА ОСНОВІ МОЛІБДЕНУ В ЗМІШАНІЙ (C_2H_2+N_2) АТМОСФЕРІ

О.В. Соболь, А.О. Андрєєв, Р.П. Мігущенко, В.М. Береснєв, А.О. Мейлехов, Г.О. Постельнік, С.О. Кравченко, Taha A. Tabaza, Safwan M. Al-Qawabah, Ubeidulla F. Al-Qawabeha, В.А. Столбовой, І.В. Сердюк, Д.А. Колесніков, М.Г. Ковалева

Для вакуумно-дугових покриттів на основі молібдену досліджено вплив тиску змішаної газової атмосфери (80%C_2H_2+20%N_2) і високовольтного негативного потенціалу (подається на підкладку в імпульсної формі) на елементний і фазовий склад, структуру і фізико-механічні характеристики формованого матеріалу. Показано, що в температурному інтервалі підкладки при осадженні 400…550 °С в результаті плазмохімічних реакцій максимальний вміст атомів азоту в покритті не перевищує 1,5 ат.%. Виявлено, що при найбільшому тиску $P_{C_2H_2+N_2} = 2{,}3\cdot10^{-1}$ Па, коли формується фаза γ-MoC, досягається надтверде стан 50,5 ГПа (при постійному потенціалі -200 В, без додаткового високовольтного імпульсного потенціалу) і 51,1 ГПа (при постійному потенціалі -200 В, з додатковим високовольтним імпульсним потенціалом).